

## Powder dynamics in very high frequency silane plasmas

J.-L. Dorier, Ch. Hollenstein, and A. A. Howling

Centre de Recherches en Physique des Plasmas, EPFL, 21 Av. des Bains CH-1007 Lausanne, Switzerland

U. Kroll

Institut de Microtechnique, 2 Rue Bréguet, CH-2000 Neuchâtel, Switzerland

Particulate contamination produced during plasma-assisted deposition of amorphous silicon devices can be responsible for reduced quality and yield. The threshold for powder formation imposes an upper limit on the radio frequency (rf) power and hence the deposition rate. In this work, the parallel-plate capacitor discharge volume is illuminated and global, spatio-temporal powder dynamics are recorded by CCD camera for analysis. The onset of powder production is determined visually and from observed modifications to the discharge electrical properties such as the matching condition, the direct current self-bias and the rf power transfer efficiency. A systematic study has been made of the powder-free operational space as a function of rf power, rf frequency (13.56–70 MHz) and substrate temperature.

### I. INTRODUCTION

Powder formation during plasma-enhanced chemical vapor deposition (PECVD) is a source of contamination to be eliminated. On the other hand, the plasma synthesis of ultrafine, high-purity microparticles has potential in the fields of ceramics and catalyzers.

Since the work of Spears,<sup>1-3</sup> powder formation in silane plasmas used for amorphous silicon (*a*-Si:H) deposition has been intensively studied.<sup>4-7</sup> In most cases, the particles are detected by laser scattering, and spatial resolution is obtained by displacing the optical system or the reactor. A global visualisation of particles in etching plasmas has been obtained by CCD camera and laser rastering.<sup>8</sup> In all cases, negatively charged particles suspended in the plasma accumulate near the plasma sheaths. Besides electrostatic forces, the particles are subject to thermophoresis forces<sup>9</sup> in the presence of any gas temperature gradient as well as viscous forces in the gas flow.<sup>4</sup> In addition, recent theoretical work has shown that charged particles can modify the electron energy distribution by Coulomb collisions and electron attachment,<sup>10</sup> and introduce recombination centres.<sup>11</sup>

In this article, powder is observed by means of white light illumination of the reactor volume for pure silane plasmas.<sup>5</sup> The global, spatio-temporal evolution of the powder is recorded and digitized by CCD camera for qualitative analysis. Modifications to the electrode voltage also serve as a powder diagnostic. After a description of the experiment, the results are presented in the following order: Section III discusses the powder influence on electrical measurements such as plasma conductance, power transfer to the plasma and electrode self-bias; Section IV is concerned with the temperature and frequency parameter space for powder-free operation. Section V describes the dependence of powder profiles on electrode temperature and excitation frequency from 13.56 to 70 MHz.

### II. EXPERIMENTAL ARRANGEMENT

The reactor (Fig. 1) consists of two, symmetric stainless steel cylindrical electrodes of diameter 130 mm positioned

20 mm apart. The gas inlet is in the side wall of the cubic vacuum chamber of side 400 mm. For these experiments, the silane flow was 30 sccm with a pressure of 0.3 mbar feedback controlled by means of a capacitance barometer acting upon the turbopump speed.

The 8×8 cm glass substrate is held by a steel template to the underside of the upper, grounded electrode which can be heated to 250 °C. The lower, radio frequency (rf) electrode can be water cooled and has a grounded guard screen. The rf power from a wideband (10 kHz–200 MHz) amplifier is capacitatively coupled to the rf electrode via a  $\pi$ -matching network at the input of which the forward and reflected rf power is measured with a directional coupler. The reactor walls are grounded and maintained at 100 °C.

A passive, rf voltage probe ( $\div 100$ ) is positioned inside the lower cylinder and contacts the back surface of the rf electrode exposed to the plasma. The voltage waveform is monitored on an electrically floating oscilloscope.

The reactor volume is illuminated with white light and observed at 90° by eye or CCD camera.<sup>5</sup> The windows are positioned at the end of 220 mm-long radial ports which suffices to eliminate any deposition which would otherwise falsify intensity measurements.

### III. THE INFLUENCE OF POWDER ON PLASMA ELECTRICAL PROPERTIES

The voltage measurement made directly on the rf electrode, in conjunction with the total input power, can be used to estimate the effective power dissipated in the plasma by a subtractive method.<sup>12-14</sup> By this method, the plasma power is given by the difference between the input power without plasma and the input power with plasma, on condition that the measurements are made at constant electrode voltage by adjustment of the amplifier output level.

Figure 2(a) shows the square of the rms electrode voltage as a function of input power, measured with plasma ( $P_{\text{tot}}$ ) and without plasma ( $P_0$  in vacuum). The reciprocal slope of the vacuum line can be equated with the circuit

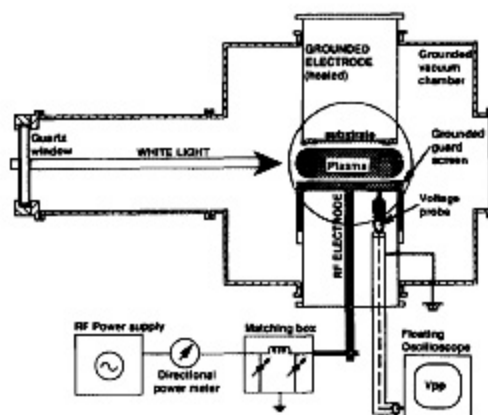


FIG. 1. Schematic of experimental arrangement showing rf circuit, electrode voltage probe, and white light illumination.

equivalent conductance  $G_0$  (real part of the admittance) as measured at the voltage probe position<sup>14</sup> using the following relation:

$$P_0 = G_0 V_{rms}^2$$

$G_0$  is observed to be a constant as expected for a linear circuit. The conductance with plasma  $G_{0k}$  is approximately independent of input power for a powder-free plasma [denoted by the unshaded region in Fig. 2(a)]. This can be understood by a simple calculation which shows that plasma conductance is approximately independent of electron density. Further evidence of constant plasma impedance is that the matching condition for zero reflected power, as determined by the value of the variable capacitors in the  $\pi$  network, is independent of input power in the absence of powder formation.

As the input power is increased, a threshold level [ $P_{thres}$  in Fig. 2(a)] is reached at which the discharge parameters change spontaneously. This threshold power and the duration of the change are reproducible for given discharge initial conditions. During this transition, the rf voltage falls steadily and the matching condition is perturbed, i.e., the reflected power increases. No particles can be seen at the onset of these electrical modifications, presumably because their size and number density are too small to be visually detected. However, as the transition continues, visible particles always appear subsequent to the electrode voltage changes at the threshold power. Powder is first seen to accumulate near the lower, rf electrode edge where the electric fringing fields to the grounded guard screen are most concentrated. The powder formation then spreads towards the axis, eventually forming a suspended disc at the plasma/sheath boundary of the rf electrode. At all times, powder streams continuously radially outwards to form an orange/yellow deposit on the side walls and the chamber floor. The deposited particles have been analysed by centrifuge and scanning electron microscopy and found

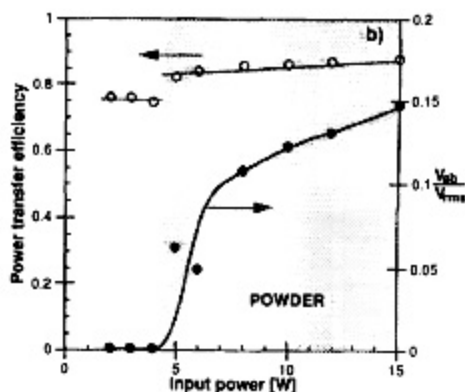
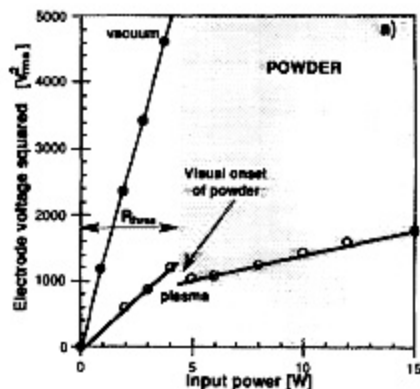


FIG. 2. Influence of powder on electrical properties of the discharge such as (a) rf electrode rms voltage squared; (b) power transfer efficiency and ratio of dc self-bias ( $V_{dc}$ ) to rf voltage (rf frequency 30 MHz, upper electrode temperature 200°C, lower electrode 15°C).

to be about 0.3  $\mu\text{m}$  in diameter. Submicron particles are thus visually detectable, although their number density, for the conditions investigated here, is higher than usually found in plasma deposition reactors.<sup>5</sup> Once the powder evolution has reached steady state, the rf voltage and reflected power levels are also stabilized. The break in the plasma line of Fig. 2(a) corresponds to this transition which lasts from 0.5 to 20 s or more, depending on the pressure, inter-electrode spacing, rf frequency and electrode temperatures.

These electrical modifications correspond to an alteration in discharge impedance due to the powder formation. From the reduction in slope, the total conductance has substantially increased for the case in Fig. 2(a). An increase in conductance, the real part of the admittance, can be explained by a diminution of the phase angle between rf current and voltage; such a phase reduction has been re-

ported for silane/argon plasmas<sup>4</sup> and diverse "dusty" plasmas.<sup>9</sup>

If we define the rf power transfer efficiency for our device to be the ratio of plasma power to total input power, it can be seen from Fig. 2(a) that this fraction is higher for the plasma-powder ensemble than for the powder-free plasma—this is shown explicitly in Fig. 2(b). Numerical calculations<sup>10</sup> show that an effect of charged particles in plasmas is to shift the electron energy distribution towards lower energies by Coulomb scattering and attachment. The increase in power transfer fraction from the electric field to the plasma-powder ensemble is thus explained by the higher cross section for electron energy loss due to trapped particles in the discharge. However, although the power transfer fraction may be higher, this is to the detriment of the required plasma processes such as dissociation and ionization because the content of high energy electrons in the tail of the distribution is reduced.

When the power is raised still further above the threshold value, the large quantity of powder produced eventually absorbs all the high energy electron content, thus stopping ionization and the plasma is extinguished.

Trapped particles also influence the direct current (dc) self-bias ( $V_{\text{dc}}$ ) of the rf electrode. Self-bias depends on the ratio of the grounded and rf electrode effective areas for plasma current flow and is negative if the rf electrode area is less than the grounded electrode surface.<sup>15</sup> In the absence of powder, the self-bias for silane plasmas in our reactor is zero or slightly negative, as expected for symmetric electrodes in a grounded vacuum chamber: the mean-free path of electrons is small enough to prevent significant leakage of plasma current outside of the electrode gap to the grounded chamber walls. With powder, however, the self-bias becomes positive; this observation has previously been attributed to the presence of negative ions.<sup>7</sup> In our case, we attribute the positive self-bias to the influence of powder which generally accumulates at the sheath in front of the cold rf electrode (see Sec. V): the negatively charged powder particles have the effect of reducing the local free electron density and energy, and consequently the self-bias must rise in order to maintain equilibrium between electron and ion currents across the rf electrode sheath.

#### IV. OPERATION DIAGRAMS FOR POWDER-FREE PLASMAS

In this section, the parameter space for powder-free plasma operation in our reactor geometry is plotted out by measuring the plasma power threshold as a function of electrode temperature and rf frequency. This threshold defines the boundary between powder-free plasma and plasma in which powder forms. The threshold power is determined by the power at which electrical discharge parameters change; this also marks the subsequent evolution of visible powder. The minimum detectable size, as described in the previous section, is at least as small as 0.3  $\mu\text{m}$ .

Figure 3 shows the plasma power threshold as a function of substrate temperature with the rf electrode main-

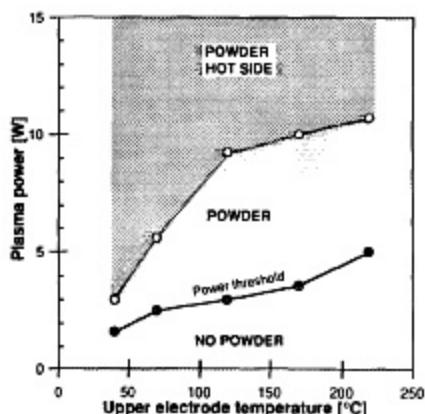


FIG. 3. Heated electrode temperature dependence of plasma power threshold for powder onset near the rf electrode at 50 °C (powder) and for the appearance of powder near the heated electrode (powder hot side), rf 50 MHz.

tained at 50 °C. No visible powder is produced for low plasma power. As the power is increased, a threshold is crossed for which powder forms at the sheath of the lower, rf electrode which is cooler than the upper, grounded electrode holding the substrate. Note that, even for equal electrode temperatures of 50 °C, the powder initially forms at the rf electrode because of the electric fringing fields to the grounded guard screen which create a local concentration of power density, thereby reducing the plasma power threshold level at the rf electrode with respect to the upper, grounded electrode. If the power is further increased beyond the threshold level in our reactor, a second power limit is reached for which powder also begins to accumulate at the substrate sheath edge (Fig. 3). At this second power limit, powder formation always begins directly opposite the junction of the glass substrate and the steel template holding the substrate to the ground electrode. This is probably caused by fringing fields due to the topography of the electrode surface, as reported by Selwyn<sup>16</sup> for powder trapped in etching plasmas. Careful design of the substrate holder to reduce fringing fields would help to avoid film contamination from particulates forming at the substrate sheath.

Figure 3 shows that for high substrate temperatures, higher power operation is possible before visible powder formation begins. This can be seen even more clearly in isothermal plasma experiments where powder formation is suppressed if the electrodes are sufficiently hot.<sup>4</sup> To explain powder suppression at high substrate temperature, it is necessary to consider the changes in plasma chemistry which influence powder formation in the plasma. The following argument is one attempt to account for the powder reduction at high temperature by considering the interaction of the plasma radicals with the electrode surfaces: The powder in silane plasmas is formed by agglomeration of

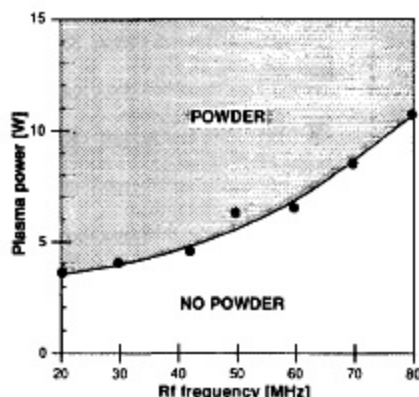


FIG. 4. rf dependence of plasma power threshold for powder onset (upper electrode temperature 200 °C, lower electrode temperature 50 °C).

certain reactive radicals (powder precursors) produced by dissociation of silane by electron impact. We can assume that radical reaction rates with the growing film surface depend on the surface temperature, because the deposition rate varies with temperature,<sup>17</sup> all else being constant. This means that the radical sticking coefficients are temperature dependent. The surface temperature, therefore, could influence the relative concentration of different dissociative products in the vicinity of the electrodes by determining which radicals are preferentially incorporated into the film, and which are less likely to stick, thereby remaining in the plasma. An explanation of the rise in power threshold with substrate temperature would then follow by postulating that the powder precursor radicals have a greater probability of sticking to the film surface at higher surface temperature, thereby lowering their concentration in the plasma and reducing the tendency to agglomerate into powder particles.

Figure 4 shows the plasma power threshold diagram for powder-free operation as a function of rf excitation frequency. Here, the upper electrode temperature is fixed at 200 °C and the lower at 50 °C. This figure illustrates the fact that higher rf frequency operation permits increased plasma power density while remaining free from particulate contamination. Sheath potentials are smaller at higher frequency for a given plasma power<sup>18</sup> and so a possible explanation is the reduction in electrostatic trapping of powder. However, it should not be discounted that very high frequency (VHF) plasma operation could also alter the relative distribution of the various dissociation products (e.g., by changing the electron energy distribution function as compared to that at 13.56 MHz) which could inhibit the production of those radicals acting as powder precursors. Some evidence to show the effect of frequency on dissociation and EEDF is the increase in deposition rate and plasma-induced emission in the VHF regime<sup>18</sup> at constant plasma power.

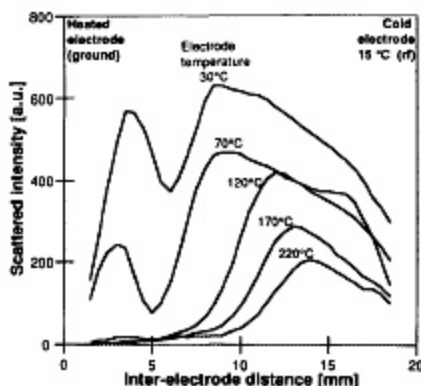


FIG. 5. Dependence of powder profiles on upper electrode temperature; the cold electrode is maintained at 15 °C (rf frequency 30 MHz, plasma power 6.4 W<sub>eff</sub>).

## V. POWDER PROFILES AS A FUNCTION OF TEMPERATURE AND rf FREQUENCY

Spatial profiles of powder formed and trapped in silane plasmas were monitored and digitized with a CCD camera by illumination of the reactor volume with white light.<sup>5</sup> The scattered intensity is a convolution of the particle size and number density, but nevertheless is a useful guide to the volume of particulates in the plasma. For the experiments described in this section, the substrate temperature was varied between 30 and 220 °C by heating the upper grounded electrode, while the lower rf electrode was maintained at 15 °C. The plasma power was above the threshold value for powder production in these conditions. The dependence on rf excitation frequency in the very high frequency range was also studied from 30 to 70 MHz.

Figure 5 represents a vertical profile, near to the electrode axis, of scattered light from the powder for different substrate temperatures with the effective plasma power and rf frequency held constant. At low temperatures, two distinct powder layers were visible—it is proposed that the negatively charged particles, surrounded by positive ions, experience a potential well which traps the powder particles at the plasma/sheath boundaries.<sup>4</sup> When the temperature is increased, the total scattered intensity is reduced and the profile is displaced towards the cold electrode. For substrate temperatures above 120 °C there is no longer any powder at the substrate sheath.

These profile modifications can be explained in terms of the change in plasma chemistry described in Sec. IV whereby the rate of formation of particles is reduced in the neighborhood of the hot electrode. However, once particles are present, the thermophoresis force<sup>9</sup> (by which a temperature gradient in the gas causes particles to move towards the cold electrode by momentum transfer of hot gas molecules to the particles) also has to be taken into account. The thermophoresis effect is observed in the following way in our reactor: First, a steady-state condition with

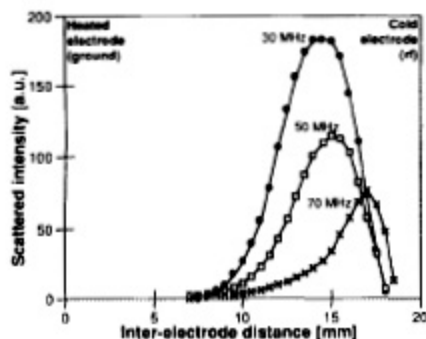


FIG. 6. Dependence of powder profiles on rf frequency (plasma power constant at 5 W<sub>eff</sub>, heated electrode temperature 220 °C, bottom electrode 15 °C).

two powder layers is established in the silane plasma. Then, when the ground electrode temperature is increased, some particles which were previously trapped near the ground electrode sheath are seen to cross the electrode gap to become trapped in the rf electrode sheath. Therefore, for a sufficiently high temperature gradient (around 80 °C/cm), the thermophoresis force appears strong enough to overcome the electric forces acting to hold particles at the substrate sheath/plasma boundary, and displace them to the rf electrode sheath/plasma boundary. Further experiments would be necessary to distinguish the relative importance of the thermophoresis force and the plasma chemistry effects in determining the powder profiles because the silane plasma is at the same time the particle source and the medium in which they are suspended.

Figure 6 shows vertical profiles of scattered light for different rf excitation frequencies at constant plasma effective power. The electrode temperatures are fixed at values where all the powder accumulates at the cold rf electrode sheath as described above. The total scattered intensity and the layer width both diminish as the frequency is increased. The sheath width, as judged by the gap between the electrode and the powder layer, is also reduced at high frequencies. As mentioned in Sec. IV, a reduction in trapping potentials, or a modification to the dissociated radical composition with VHF operation are possible explanations for these frequency-dependent phenomena.

The above measurements were all made with continuous, constant amplitude rf power. Another important technique for powder suppression is by using rf power modulation at kiloHertz frequencies,<sup>5,6</sup> or intermittent pulsed rf power.<sup>4</sup> This method, combined with high substrate temperature and frequency, could allow still larger plasma power densities with no powder formation with a corresponding increase in deposition rate of high-quality films.

## VI. CONCLUSIONS

The problem of powder contamination in plasma deposition reactors has been investigated. We discuss the tran-

sition from powder-free to powder-producing plasmas, during which the discharge voltage, plasma conductance, power transfer fraction, and rf electrode dc self-bias all change spontaneously. This transition defines a maximum power threshold for powder-free plasma.

High substrate temperature and high rf excitation frequency both have the effect of raising the power threshold, allowing a higher power density and thereby increased deposition rate without powder contamination. It is suggested that this could be due to a change in radical composition in both cases, inhibiting the development of powder precursors in the discharge.

If conditions are such that powder forms in the plasma, thermophoresis forces<sup>9</sup> due to the presence of a temperature gradient can play a role in determining the spatial distribution of powder; e.g., by displacing particles away from a hot substrate to a colder counter-electrode. Furthermore, the discharge electric fields and therefore the electric trapping potentials are diminished by high frequency operation, which could reduce the tendency for powder to accumulate in the plasma.

From the point of view of powder contamination reduction, plasma operation at high substrate temperature and high frequency are both seen to be beneficial.

## ACKNOWLEDGMENTS

This work was funded by Swiss Federal Research Grants BB.WEG(91)3 (for BRITE/EURAM Contract No. BE-4529-90) and EF-REN(89)17.

<sup>1</sup>K. G. Spears, T. J. Robinson, and R. M. Roth, *IEEE Trans. Plasma Sci.* **14**, 179 (1986).

<sup>2</sup>K. G. Spears, R. P. Kampf, and T. J. Robinson, *J. Chem. Phys.* **92**, 5297 (1987).

<sup>3</sup>K. G. Spears and T. J. Robinson, *J. Chem. Phys.* **92**, 5302 (1987).

<sup>4</sup>A. Bouchoule, A. Plain, L. Boufendi, J.-Ph. Blondeau, and C. Laure, *J. Appl. Phys.* **70**, 1991 (1991).

<sup>5</sup>A. A. Howling, Ch. Hollenstein, and P.-J. Paris, *Appl. Phys. Lett.* **59**, 1409 (1991).

<sup>6</sup>Y. Watanabe, M. Shiratani, and H. Makino, *Appl. Phys. Lett.* **57**, 1616 (1990).

<sup>7</sup>F. J. Kampus and M. J. Kushner, *IEEE Trans. Plasma Sci.* **14**, 173 (1986).

<sup>8</sup>G. S. Selwyn, J. E. Heidenreich, and K. L. Haller, *Appl. Phys. Lett.* **57**, 1876 (1990).

<sup>9</sup>G. M. Jellum, J. E. Daugherty, and D. B. Graves, *J. Appl. Phys.* **69**, 6923 (1991).

<sup>10</sup>M. J. McCaughey and M. J. Kushner, *Appl. Phys. Lett.* **55**, 951 (1989); *J. Appl. Phys.* **69**, 6952 (1991).

<sup>11</sup>A. Garscadden, *Nonequilibrium Processes in Partially Ionized Gases*, edited by M. Capitelli and J. N. Bardsley (Plenum, New York, 1990), p. 541.

<sup>12</sup>J. S. Logan, in *Handbook of Plasma Processing Technology*, edited by S. M. Rossnagel, J. J. Cuomo, and W. D. Westwood (Noyes, Park Ridge, NJ, 1990), p. 155.

<sup>13</sup>C. M. Horwitz, *J. Vac. Sci. Technol. A* **1**, 1795 (1983).

<sup>14</sup>V. A. Godysak and R. B. Pejak, *J. Vac. Sci. Technol. A* **8**, 3833 (1990).

<sup>15</sup>K. Köhler, D. E. Hone, and J. W. Coburn, *J. Appl. Phys.* **58**, 3350 (1985).

<sup>16</sup>G. S. Selwyn, *J. Vac. Sci. Technol. A* **7**, 2758 (1989).

<sup>17</sup>J.-L. Andujar, E. Bertran, A. Canillas, J. Campmany, and J. L. Morozu, *J. Appl. Phys.* **69**, 3757 (1991).

<sup>18</sup>A. A. Howling, J.-L. Dorier, Ch. Hollenstein, U. Kroll, and F. Finger, *J. Vac. Sci. Technol. A* **10**, 1080 (1992).